

Theoretical investigation of differences in nitroreduction of aristolochic acid I by cytochromes P450 1A1, 1A2 and 1B1

Petr JERABEK, Vaclav MARTINEK, Marie STIBOROVA

Department of Biochemistry, Faculty of Science, Charles University, Prague, Czech Republic

Correspondence to: Prof. RNDr. Marie Stiborova, DSc.
Department of Biochemistry, Faculty of Science, Charles University in Prague,
Albertov 2030, 128 40 Prague 2, Czech Republic.
TEL: +420-221951285; FAX: +420-221951283; E-MAIL: stiborov@natur.cuni.cz

Submitted: 2012-09-01 *Accepted:* 2012-11-15 *Published online:* 2012-12-26

Key words: **aristolochic acid; aristolochic acid nephropathy; Balkan endemic nephropathy; cytochromes P450 1A1, 1A2 and 1B1, metabolic activation; molecular modeling**

Neuroendocrinol Lett 2012;33(Suppl.3):25–32 PMID: 23353840 NEL330912A03 ©2012 Neuroendocrinology Letters • www.nel.edu

Abstract

OBJECTIVES: The herbal drug aristolochic acid (AA) derived from *Aristolochia* species has been shown to be the cause of aristolochic acid nephropathy (AAN), Balkan endemic nephropathy (BEN) and their urothelial malignancies. One of the common features of AAN and BEN is that not all individuals exposed to AA suffer from nephropathy and tumor development. One cause for these different responses may be individual differences in the activities of the enzymes catalyzing the biotransformation of AA. Thus, the identification of enzymes principally involved in the metabolism of AAI, the major toxic component of AA, and detailed knowledge of their catalytic specificities is of major importance. Human cytochrome P450 (CYP) 1A1 and 1A2 enzymes were found to be responsible for the AAI reductive activation to form AAI-DNA adducts, while its structurally related analogue, CYP1B1 is almost without such activity. However, knowledge of the differences in mechanistic details of CYP1A1-, 1A2-, and 1B1- mediated reduction is still lacking. Therefore, this feature is the aim of the present study.

METHODS: Molecular modeling capable of evaluating interactions of AAI with the active site of human CYP1A1, 1A2 and 1B1 under the reductive conditions was used. *In silico* docking, employing soft-soft (flexible) docking procedure was used to study the interactions of AAI with the active sites of these human enzymes.

RESULTS: The predicted binding free energies and distances between an AAI ligand and a heme cofactor are similar for all CYPs evaluated. AAI also binds to the active sites of CYP1A1, 1A2 and 1B1 in similar orientations. The carboxylic group of AAI is in the binding position situated directly above heme iron. This ligand orientation is in CYP1A1/1A2 further stabilized by two hydrogen bonds; one between an oxygen atom of the AAI nitro-group and the hydroxyl group of Ser122/Thr124; and the second bond between an oxygen atom of dioxolane ring of AAI and the hydroxyl group of Thr497/Thr498. For the CYP1B1:AAI complex, however, any hydrogen bonding of the nitro-group of AAI is prevented as Ser122/Thr124 residues are in CYP1B1 protein replaced by hydrophobic residue Ala133.

CONCLUSION: The experimental observations indicate that CYP1B1 is more than 10× less efficient in reductive activation of AAI than CYP1A2. The docking simulation however predicts the binding pose and binding energy of AAI in the CYP1B1 pocket to be analogous to that found in CYP1A1/2. We believe that the hydroxyl

group of S122/T124 residue, with its polar hydrogen placed close to the nitro group of the substrate (AAI), is mechanistically important, for example it could provide a proton required for the stepwise reduction process. The absence of a suitable proton donor in the AAI-CYP1B1 binary complex could be the key difference, as the nitro group is in this complex surrounded only by the hydrophobic residues with potential hydrogen donors not closer than 5 Å.

Abbreviations:

AA	- aristolochic acid
AAI	- aristolochic acid I [8-methoxy-6-nitro-phenanthro-(3,4-d)-1,3-dioxolo-5-carboxylic acid]
AAIa	- aristolochic acid Ia [8-hydroxy-6-nitro-phenanthro-(3,4-d)-1,3-dioxolo-5-carboxylic acid]
AAII	- 6-nitro-phenanthro-(3,4-d)-1,3-dioxolo-5-carboxylic acid
AAN	- aristolochic acid nephropathy
AlaI	- aristolactam I
Å	- Angstrom
BEN	- Balkan endemic nephropathy
CYP	- cytochrome P450
dA-AAI	- 7-(deoxyadenosin- <i>N</i> ⁶ -yl)aristolactam I
dA-AAII	- 7-(deoxyadenosin- <i>N</i> ⁶ -yl)aristolactam II
dG-AAI	- 7-(deoxyguanosin- <i>N</i> ² -yl) aristolactam I
NADPH	- nicotinamide adenine dinucleotide phosphate (reduced)
NQO1	- NAD(P)H:quinone oxidoreductase
PDB	- Protein Data Bank
POR	- NADPH:cytochrome P450 oxidoreductase
RAL	- relative adduct labeling
RMSD	- root-mean-square deviation
SULT	- sulfotransferase
NAT	- <i>N,O</i> -acetyltransferase
UUC	- upper urinary tract urothelial carcinoma
WT	- wild-type

INTRODUCTION

The herbal drug aristolochic acid (AA) derived from *Aristolochia* species has been shown to be the cause of so-called Chinese herbs nephropathy, now termed aristolochic acid nephropathy (AAN) (DeBelle *et al.* 2008; Schmeiser *et al.* 2009). The plant extract AA is a mixture of structurally related nitrophenanthrene carboxylic acids, the major components being aristolochic acid I (AAI) and aristolochic acid II (AAII).

AAN is a rapidly progressive renal fibrosis that was initially observed in a group of Belgian women who had ingested weight loss pills containing *Aristolochia fangchi* (Vanherweghem *et al.* 1993; Nortier *et al.* 2000). Within a few years of taking the pills, AAN patients also showed a high risk (~50%) of upper urothelial tract carcinoma and, subsequently, bladder urothelial carcinoma. In the meantime, similar cases have been reported elsewhere in Europe and Asia (Schmeiser *et al.* 2009). Dietary exposure to AA has also been linked to Balkan endemic nephropathy (BEN) and its associated urothelial cancer (Arlt *et al.* 2007; Grollman *et al.* 2007; Moriya *et al.* 2011); this nephropathy is endemic in certain rural areas of Serbia, Bosnia, Croatia, Bulgaria and Romania.

Exposure to AA was demonstrated by identification of specific AA-DNA adducts in urothelial tissue of AAN and BEN patients (Schmeiser *et al.* 1996; Nortier *et al.* 2000; Arlt *et al.* 2002; Grollman *et al.* 2007; Jelaković *et al.* 2012; Yun *et al.* 2012). The most abundant DNA adduct detected in patients is 7-(deoxyadenosin-*N*⁶-yl) aristolactam I (dA-AAI) (Figure 1), which causes characteristic AT→TA transversions. Such AT→TA mutations have been observed in the *TP53* tumor suppressor gene in tumors from AAN and BEN patients (Lord *et al.* 2004; Grollman *et al.* 2007; Moriya *et al.* 2011), indicating a probable molecular mechanism associated with AA-induced carcinogenesis (Arlt *et al.* 2007; Kucab *et al.* 2010). More recently, AA exposure was discovered to contribute to the high incidence of upper urinary tract urothelial carcinoma (UUC) in Taiwan, where medicinal use of *Aristolochia* plants is widespread (Chen *et al.* 2012); again, the *TP53* mutational signature in patients with UUC was predominant among otherwise rare AT→TA transversions (Olivier *et al.* 2012). AA has been classified as a Group I carcinogen in humans by the International Agency for Research on Cancer (Grosse *et al.* 2009).

The activation pathway for AAI is nitroreduction, catalyzed by both cytosolic and microsomal enzymes; in this process NAD(P)H:quinone oxidoreductase (NQO1) is the most efficient cytosolic nitroreductase (Stiborova *et al.* 2003, 2008a, 2008b; Chen *et al.* 2011; Martinek *et al.* 2011) (Figure 1). In contrast to NQO1, conjugation enzymes such as human sulfotransferases (SULTs) or *N,O*-acetyltransferases (NATs) did not significantly activate AAI (Martinek *et al.* 2011; Stiborova *et al.* 2011a) (Figure 2). In human hepatic microsomes, AAI is activated by cytochrome P450 1A2 (CYP1A2) and, to a lesser extent, by CYP1A1; P450 oxidoreductase (POR) also plays a minor role (Stiborova *et al.* 2001, 2005). Of human recombinant CYP enzymes, CYP1A2, followed by CYP1A1 are the most effective to reductively activate AAI, while other CYPs are almost ineffective in this reaction (Stiborova *et al.* 2005) (Figure 2). Human and rodent CYP1A1 and 1A2 are also the principal enzymes involved in oxidative detoxication of AAI to 8-hydroxyaristolochic acid I (aristolochic acid Ia, AAIIa) (Sistkova *et al.* 2008; Shibutani *et al.* 2010; Stiborova *et al.* 2011b; 2012).

The role of cytochrome P450 enzymes, particularly CYP1A1 and CYP1A2, both in the reductive activation and oxidative detoxication of AAI, was demonstrated in several animal studies. Two studies used the Hepatic P450 Reductase Null (HRN) mice - in which the *Por* gene is deleted specifically in hepatocytes - resulting in absence of CYP activity (Xiao *et al.* 2008; Levová *et al.* 2011), four others used *Cyp1a1*(-/-), *Cyp1a2*(-/-) and/or *Cyp1a1/1a2*(-/-) and CYP1A-humanized mouse lines (Rosenquist *et al.* 2010; Arlt *et al.* 2011; Stiborova *et al.* 2012).

Overall, AAI-DNA adduct levels were higher in CYP1A-humanized mice than in wild-type (WT) mice,

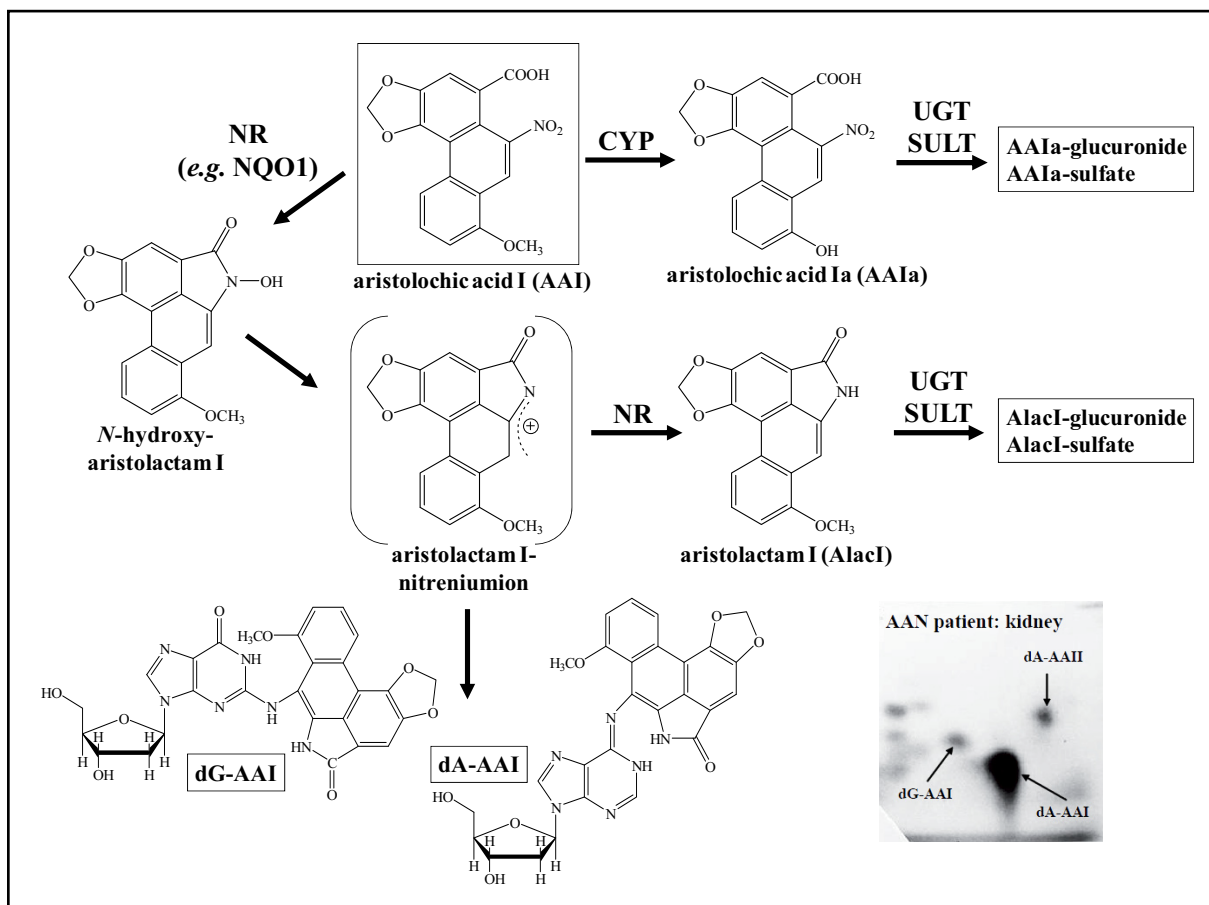


Fig. 1. Pathways of biotransformation and DNA adduct formation of AAI. dA-AAI, 7-(deoxyadenosin-*N*⁶-yl)aristolactam I; dG-AAI, 7-(deoxyguanosin-*N*²-yl)aristolactam I; NR, nitro-reduction; UGT, UDP glucuronosyltransferase; SULT, sulfotransferase. Insert: Autoradiographic profile of AAI-DNA adducts found in kidney of AAN patients.

suggesting strongly that human CYP1A1 and 1A2 causes higher AAI bioactivation than mouse CYP1A1 and CYP1A2 (Stiborova *et al.* 2012).

In contrast to the mechanism responsible for oxidation (hydroxylation) reactions catalyzed by CYP enzymes that has been partially explained (Schyman *et al.* 2011), information on the mechanism of nitroreduction catalyzed by these enzymes is still lacking. Therefore, this feature is the aim of the present study. Another aim of this study is to explain the reason(s) why only CYP1A1 and 1A2 are effective in nitroreduction of AAI, while its structurally similar analogue, CYP1B1 is almost without such activity (Figure 2). Molecular modeling capable of evaluating interactions of AAI with the active site of human CYP1A1, 1A2 and 1B1 under the reductive conditions was used for such a study.

MATERIALS AND METHODS

Homology modeling of human CYP1A1

To date, there is no three-dimensional structures of CYP1A1 deposited in PDB databank, however the structure of highly homologous protein human

CYP1A2 is available (PDB ID 2HI4) (Sansen *et al.* 2007). Therefore, we decided to use homology modeling to create a model of soluble domain of human CYP1A1 with human CYP1A2 as a template, because the soluble domains of both enzymes have 85% homology. For sequence alignment of the truncated human CYP1A2 with human CYP1A1, see Figure 3. The model of soluble domain of human CYP1A1, including residues 32–509, was generated using server SWISS-MODEL (Schwede *et al.* 2003). The model was evaluated using program PROCHECK v3.4 (Laskowski *et al.* 1993) and showed acceptable quality. 88.2% residues were in most favored regions, 10.3% in additional allowed regions and 3 glycine residues were in generously allowed regions. Residues L48, S116 and S303 were found in disallowed regions, but they are positioned on the surface, out of a region treated as flexible during docking. L48, S116 were found in disallowed regions also in the template structure (CYP1A2) and their anomalous placement could be related to the fact that native CYP1A1 and 1A2 are membrane proteins. The last problematic residue S303 corresponding to P303 of the template is located in the surface loop more

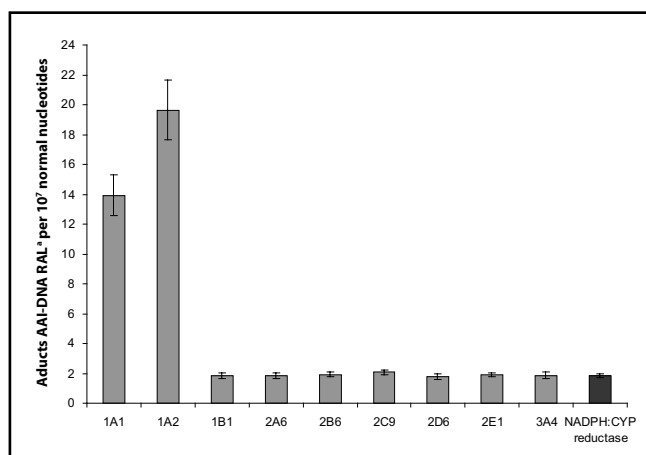


Fig. 2. AAI-DNA adduct formation by human CYP enzymes in Supersomes™. Data are taken from Stiborova *et al.* (2005).



Fig. 3. The sequence of truncated human CYP1A2 (Query) aligned with human CYP1A1 (Subject).

than 24 Å from the active site. Side chains of all residues interacting with the ligand and heme were conserved between the model and template.

Molecular docking of AAI into human CYP1A1, 1A2 and 1B1

The soft-soft docking procedure was similar as described previously (Stiborova *et al.* 2011a; Martinek *et al.* 2011). The X-ray based coordinates of human CYP1A2 (1.95 Å resolution, PDB ID 2HI4) (Sansen *et al.* 2007) and CYP1B1 (2.7 Å resolution, PDB ID 3PM0) (Wang *et al.* 2011) together with homologous model of human CYP1A1 were used as starting structures for modeling of AAI interactions with the ground state of CYP enzymes. During structure preparation, hydrogen atoms were added and crystallographic water and the alpha-naphthoflavone ligand molecules were removed, usual protonation states and AMBER partial charges were assigned to all residues, except for the atomic charge of the ferric ion of the heme cofactor, for which a value more consistent with a metal in octahedral coordination was used (Pontikis *et al.* 2009). The geometries

and charges of a ligand (AAI) were predicted using *ab initio* calculations on the Hartree-Fock level of theory in conjunction with the 6-31+G(d) basis set. All *ab initio* calculations were performed with program Gaussian 03 (Frisch *et al.* 2003).

We employed a hybrid global-local Lamarckian genetic algorithm implemented in modified Autodock v4.2.3 program suite (Huey *et al.* 2007) to evaluate binding free energies and preferred binding modes for studied compounds. The Autodock v4 combines two methods to find the most preferable binding modes, rapid grid-based energy evaluation and efficient search of torsional freedom, together with optional soft-soft docking. During the flexible docking procedure, both the position of the ligand and the orientations of the selected flexible side-chains are optimized simultaneously. In order to allow the enzyme to adapt to a new ligand, we ran soft-soft docking calculations. All rotatable bonds of the ligands and 10-11 selected amino acid side chains, CYP1A1 (S122, F123, N221, F224, F258, D313, D320, T321, V382, L496, T497), CYP1A2 (T124, F125, T223, F226, F260, D313, D320, T321, L382, L497, T498), CYP1B1 (F134, N228, F231, F268, D326, D333, T334, V395, L509, T510) were allowed to rotate freely. We performed an extensive search (2000 docking runs per system) of the most preferred binding modes of an AAI ligand within a 57x47x47 grid-box centered on the substrate binding cavity. Similar resulting structures (RMSD lower than 1.0 Å) were grouped and finally sorted by binding free energy of the best binding structure within each cluster. As a result, a set of binding modes with similar binding energies was obtained for every system. We assume that only the orientations with a sufficiently short distance between the electron acceptor (AAI) and an electron donor (heme) in the CYP would facilitate the reduction.

RESULTS AND DISCUSSION

Although the amino acid sequences of human CYP1A1, 1A2 and 1B1 show different levels of homology, all enzymes possess narrow active site cavities, which is reflected in their similar substrate preferences (Wang *et al.* 2011). For example 9-hydroxylation of ellipticine is catalyzed by CYP1A1, 1A2 and 1B1 at similar rates: 2.8, 2.5 and 1.6 pmol/min/nmol_{CYP} respectively (Stiborova *et al.* 2011c). However there are several substrates, whose metabolic preferences for CYP1A1, 1A2 and 1B1 vary substantially. For instance the rate of Sudan I oxidation mediated by human enzymes of a CYP1 family is high only for CYP1A1, while its oxidation by homologous CYP1A2 and CYP1B1 is more than 10-times slower (Stiborova *et al.* 2002, 2006).

The structural alignment of human CYP1A1, 1A2 and 1B1 examined here and difference in their cavities are illustrated in Figure 4. Their substrate binding cavities near the heme cofactor show higher shape resemblance than their upper parts near the substrate access

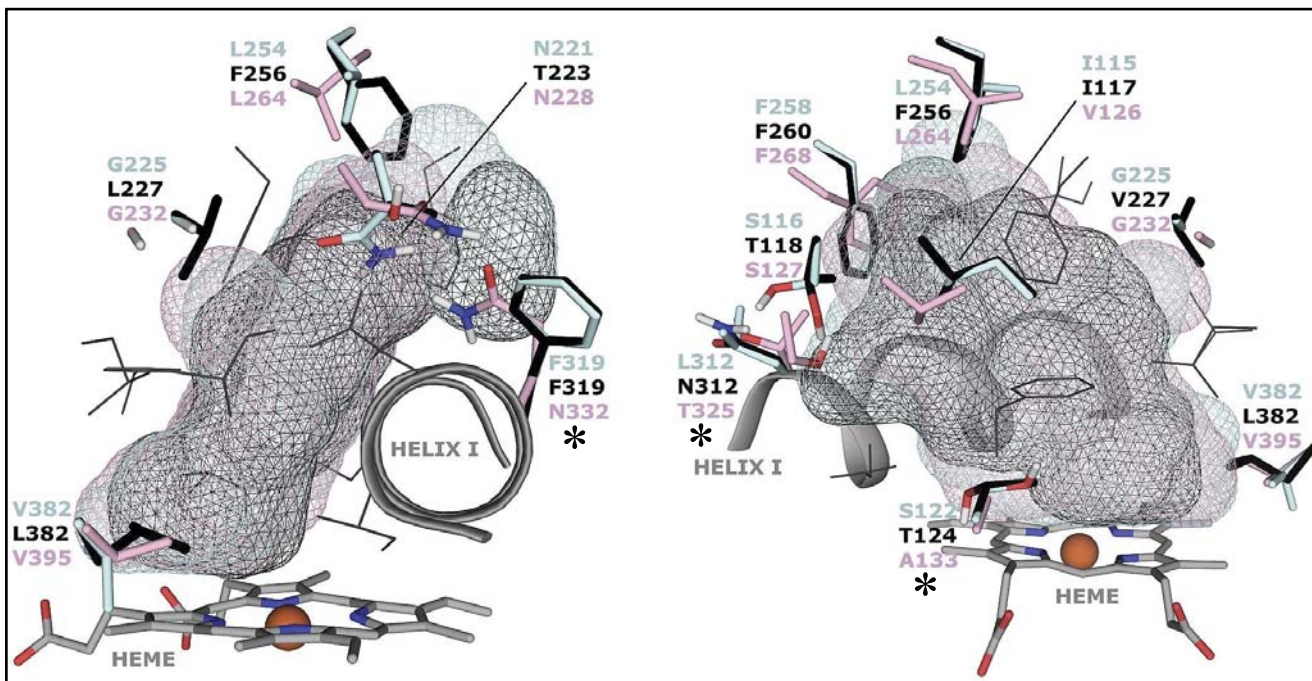


Fig. 4. Superposition of CYP1A1 (cyan), 1A2 (black) and 1B1 (pink) active sites, edge and site view. Substrate binding cavities are rendered as *mesh surfaces*. Side chains of non-conserved residues are rendered as sticks; other flexible residues are shown as lines. The major differences in side chain composition resulting in significant changes of binding site properties are marked with asterisks.

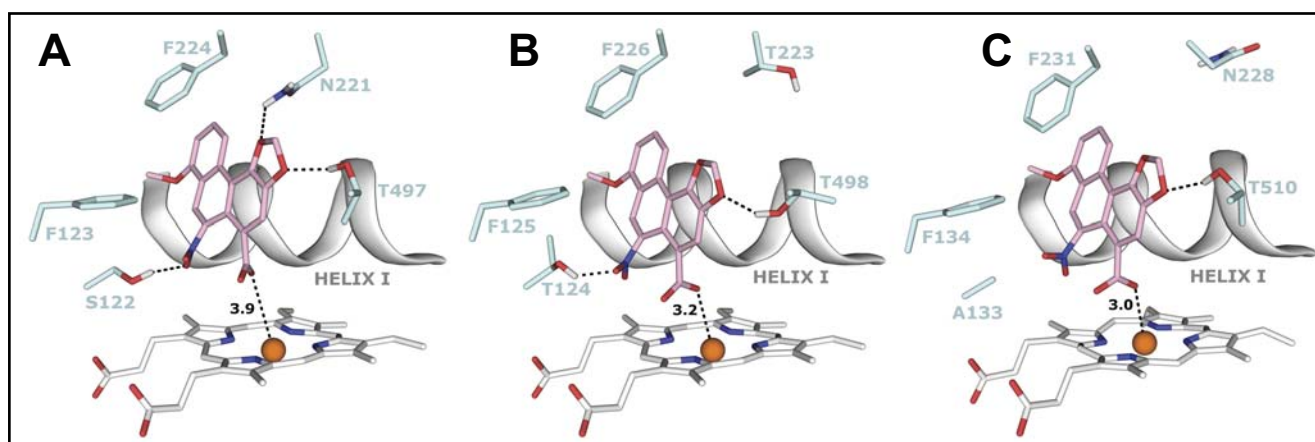


Fig. 5. The most favorable binding orientations of AAI docked into the active site of CYP1A1 (A), 1A2 (B) and 1B1 (C). Hydrogen bonds between AAI and the amino acid residues in active site residues are rendered as dashed black lines. AAI (pink), heme (grey) and side chains of important amino acid residues (cyan) are rendered as bold sticks; iron ions as orange spheres.

channel (not shown in Figure 4). One side of the binding pocket is defined by helix I and the opposite side is formed mostly by residues of hydrophobic amino acids. The only three major differences in composition of the binding cavities of CYP1A1, 1A2 and 1B1 could be recognized: (i) the presence of Leu312 in CYP1A1 in the place of polar residues Asn312/CYP1A2 or Thr325/CYP1B1, (ii) the residue Ala133 in CYP1B1 is substituting polar residues Ser122/CYP1A1 or Thr124/CYP1A2 and (iii) replacement of hydrophobic residue of Phe319 in CYP1A1/2 by a polar amino acid Asn332 in CYP1B1. Besides steric effects, these differences result in alteration of physico-chemical properties of the substrate

binding pocket of evaluated CYPs. These alterations could also contribute to variation in CYP1A1, 1A2 and 1B1 substrate preferences.

Currently no information is known about the mechanism of nitroreduction catalyzed by CYP enzymes. We suppose that the direct hydride transfer that is proposed for reduction of AAI by the nitroreductase NQO1 (Stiborova *et al.* 2011a; Martinek *et al.* 2011) is not applicable for CYPs as they lack a suitable hydride donor group in their active sites. Only the stepwise reduction mechanism (e^- , H^+ , e^- , H^+) which was proposed as alternative for reduction of AAI by NQO1 (Stiborova *et al.* 2011a; Martinek *et al.* 2011) is applicable here. We

assume that any binding conformations allowing close contacts between the electron donor (super-aromatic system of heme) and the electron acceptor (aromatic system of AAI and conjugated nitro- and carboxylic groups) would facilitate the first electron transfer. This step is presumably followed by the consequent proton transfer from an unknown donor to the nitro-group of AAI.

In order to simulate the reductive activation of AAI by CYPs, the enzyme models included the ground state form of prosthetic groups (ferric protoporphyrin IX). Binding of AAI into the ground state of CYP represents a step directly preceding nitroreduction catalyzed by CYPs under the anaerobic conditions.

Molecular docking of AAI to the active site of CYP1A1, 1A2 and 1B1

To examine the nature of differences in mechanistic details of CYP1A1-, 1A2- and 1B1-mediated reduction of AAI, the AAI binding to the active centre of these enzymes was modeled. Because the initial structure coordinates were based on CYPs co-crystallized with another ligand (α -naphthoflavone), the flexible docking procedure was employed in order to allow the CYP active site to adopt a ligand of different size and shape. During the docking procedure AAI and 10–11 amino acid side chains shaping the binding cavity were treated as flexible (Figure 4).

The most stable binding modes of AAI bound into CYP1A1, 1A2 and 1B1 predicted by flexible docking show high structural resemblance (Figure 5). Also the predicted binding free energies and distances between the AAI ligand and the heme cofactor for evaluated CYP complexes are similar (see Table 1). AAI forms the most stable complex with human CYP1A2. The AAI is in this binding pose situated in the bottom and the central part of the CYP1A2 binding pocket, with the carboxylic group of the AAI placed 3.2 Å above heme iron (Figure 5B). This ligand orientation is further stabilized by two hydrogen bonds; one between an oxygen atom of the AAI nitro-group and the hydroxyl group of Thr124; and the second bond between an oxygen atom of the dioxolane ring of AAI and the hydroxyl group

of Thr498. Similar docking poses were predicted also for CYP1A1 and 1B1 (Figure 5). Orientation of AAI in the CYP1A1 active site is almost identical with that in CYP1A2, including analogous hydrogen bonding to the corresponding residues Ser122 and Thr497, except that AAI in the CYP1A1 cavity is due to additional hydrogen bonding to Asn 221 pulled 0.7 Å farther from the heme cofactor (Figure 5A). It is possible that the longer electron transfer distance could contribute to the 30% lower rates of CYP1A1-mediated reductive activation of AAI activation in comparison to CYP1A2-mediated activation found in *in vitro* experiments (Figure 2).

The experimental observations indicate that CYP1B1 plays only a minor role in activation of AAI; the CYP1B1 is more than 10-times less efficient in activating AAI (Figure 2). The docking simulation however predicts the binding pose and binding energy of AAI in the CYP1B1 pocket to be analogous to that found in CYP1A2 (Figure 5C and Table 1). As in the CYP1A2, the oxygen atom of dioxolane ring of AAI and the hydroxyl group of Thr510 in CYP1B1 form the hydrogen bond, but the important difference is based on altered hydrogen bonding of the AAI nitro group. Residues Ser122/Thr124 that are directly interacting with the nitro group of AAI in complexes with CYP1A1/1A2, are in the CYP1B1 protein replaced by the hydrophobic residue Ala133. The absence of one hydrogen bond might result in slightly lower binding affinity of AAI toward CYP1B1 (Table 1), nevertheless this could not explain the substantial differences in AAI activation efficiency of the CYP1B1 vs. CYP1A1/2. We however believe that the hydroxyl group of Ser122/Thr124 residue, with its polar hydrogen placed close (1.9 Å) to the nitro group of the substrate (AAI), could play a role in the CYP catalyzed reduction of AAI, for example it could provide a proton required for the stepwise reduction process. The vicinity of the nitro group in the CYP1B1-AAI complex is completely hydrophobic, with potential hydrogen donors not closer than 5 Å. The hydrogen bonding between an enzyme and its substrate generally plays an important role in the enzyme catalysis and was shown to correlate with its enzymatic efficiency (Poulos, 1995; Martinek *et al.* 2007). Although the interaction of AAI with other CYPs shown in Figure 2 were not evaluated by the means of flexible molecular docking, we should note that the CYP enzymes belonging to family 2, likewise CYP1B1, contain only a hydrophobic residues (Ala, Ile, Phe or Val) in position corresponding to Ser122/Thr124. We propose that Ser122 and Thr124 could play essential role in an unusually high rate of CYP1A1 and 1A2 mediated reduction of AAI that is much faster for these two CYP enzymes in comparison to other CYPs evaluated experimentally. The experimental confirmation of the hypothesis is currently under way in our laboratory.

The difference in AAI activation preferences between CYP1B1 vs. CYP1A1/2 could be attributed also to other processes which are not directly related to

Tab. 1. The estimated binding free energies and distances between AAI ligand and heme cofactor for the best ranked complexes shown in Figure 5.

	Free energy of binding [kcal/mol]	COO-(AAI) – Fe ³⁺ (heme) distance [Å] ^a
CYP1A1	5.66	3.9
CYP1A2	5.81	3.2
CYP1B1	5.59	3.0

^a Distance between the closest oxygen atom of carboxylic group of AAI and heme iron in individual CYPs.

the AAI affinities to their binding sites. For example, it should be noted that active sites of most CYP enzymes are buried deep inside the protein globule and are accessible through a narrow access channel, the access channel is smaller than their typical substrate. Access of a substrate through this channel requires substantial flexibility of the CYP protein molecule, but unfortunately such a degree of flexibility could not be modeled using the current docking techniques.

ACKNOWLEDGEMENTS

The authors would like to thank to Grant Agency of Czech Republic (grants 301/09/0472 and 305/09/H008) and to Charles University (grant UNCE 204025/2012). The access to the MetaCentrum and CERIT-SC computing facilities provided under the programmes LM2010005 and CZ. 1.05/3.2.00/08.0144 is highly appreciated.

Potential Conflicts of Interest: None disclosed.

REFERENCES

- Arlt VM, Ferluga D, Stiborova M, Pfohl-Leszkowicz A, Vukelic M, Ceovic S, *et al.* (2002) Is aristolochic acid a risk factor for Balkan endemic nephropathy-associated urothelial cancer? *Int J Cancer* **101**: 500–502.
- Arlt VM, Levova K, Barta F, Shi Z, Evans JD, Frei E, *et al.* (2011) Role of P450 1A1 and P450 1A2 in bioactivation versus detoxication of the renal carcinogen aristolochic acid I: studies in Cyp1a1^{-/-}, Cyp1a2^{-/-}, and Cyp1a1/1a2^{-/-} mice. *Chem Res Toxicol* **24**: 1710–1719.
- Arlt VM, Stiborova M, vom Brocke J, Simões ML, Lord GM, Nortier JL, *et al.* (2007). Aristolochic acid mutagenesis: molecular clues to the aetiology of Balkan endemic nephropathy-associated urothelial cancer. *Carcinogenesis* **28**: 2253–2261.
- Debelle FD, Vanherweghem J-L and Nortier JL (2008) Aristolochic acid nephropathy: a worldwide problem. *Kidney Int* **74**: 158–169.
- Frisch M, Trucks GW, Schlegel HB, Robb MA and Cheeseman JR (2003) Gaussian 03. Wallingford, CT, USA: Gaussian Inc.
- Grollman AP, Shibusatani S, Moriya M, Miller F, Wu L, Moll U, *et al.* (2007) Aristolochic acid and the etiology of endemic (Balkan) nephropathy. *Proc Natl Acad Sci USA* **104**: 12129–12134.
- Grosse Y, Baan R, Straif K, Secretan B, El Ghissassi F, Bouvard V, Benbrahim-Tallaa L, Guha N, Galichet L, Cogliano V (2009) A review of human carcinogens-Part A: pharmaceuticals. *Lancet Oncol* **10**: 13–14.
- Huey R, Morris GM, Olson AJ and Goodsell DS (2007) A semiempirical free energy force field with charge-based desolvation. *J Comput Chem* **28**: 1145–1152.
- Chen C-H, Dickman KG, Moriya M, Zavadil J, Sidorenko VS, Edwards KL, *et al.* (2012) Aristolochic acid-associated urothelial cancer in Taiwan. *Proc Natl Acad Sci USA* **109**: 8241–8246.
- Chen M, Gong L, Qi X, Xing G, Luan Y, Wu Y, *et al.* (2011) Inhibition of renal NQO1 activity by dicoumarol suppresses nitroreduction of aristolochic acid I and attenuates its nephrotoxicity. *Toxicol Sci* **122**: 288–296.
- Jelaković B, Karanović S, Vuković-Lela I, Miller F, Edwards KL, Nikolić J, *et al.* (2012) Aristolactam-DNA adducts are a biomarker of environmental exposure to aristolochic acid. *Kidney Int* **81**: 559–567.
- Kucab JE, Phillips DH, Arlt VM (2010) Linking environmental carcinogen exposure to TP53 mutations in human tumours using the human TP53 knock-in (Hupki) mouse model. *FEBS J* **277**: 2567–2583.
- Levova K, Moserova M, Kotrbova V, Sulc M, Henderson CJ, Wolf CR, Phillips DH, *et al.* (2011) Role of cytochromes P450 1A1/2 in detoxication and activation of carcinogenic aristolochic acid I: studies with the hepatic NADPH:cytochrome P450 reductase null (HRN) mouse model. *Toxicol Sci* **121**: 43–56.
- Lord GM, Hollstein M, Arlt VM, Roufousse C, Pusey CD, Cook T, *et al.* (2004) DNA adducts and p53 mutations in a patient with aristolochic acid-associated nephropathy. *Am J Kidney Dis* **43**: e11–17.
- Martinek V, Bren U, Goodman MF, Warshel A and Florian J (2007) DNA polymerase beta catalytic efficiency mirrors the Asn279-dCTP H-bonding strength. *FEBS Lett* **581**: 775–780.
- Martinek V, Kubickova B, Arlt VM, Frei E, Schmeiser HH, Hudecek J, *et al.* (2011) Comparison of activation of aristolochic acid I and II with NADPH:quinone oxidoreductase, sulphotransferases and N-acetyltransferases. *Neuroendocrinol Lett* **32**: 57–70.
- Moriya M, Slade N, Brdar B, Medverec Z, Tomic K, Jelaković B, Wu L, *et al.* (2011) TP53 Mutational signature for aristolochic acid: an environmental carcinogen. *Int J Cancer* **129**: 1532–1536.
- Nortier JL, Martinez MC, Schmeiser HH, Arlt VM, Bieler CA, Petein M, *et al.* (2000) Urothelial carcinoma associated with the use of a Chinese herb (Aristolochia fangchi). *N Engl J Med* **342**: 1686–1692.
- Olivier M, Hollstein M, Schmeiser HH, Straif K and Wild CP (2012) Upper urinary tract urothelial cancers: where it is A:T. *Nature Reviews Cancer* **12**: 503–504.
- Pontikis G, Borden J, Martinek V and Florián J (2009) Linear energy relationships for the octahedral preference of Mg, Ca and transition metal ions. *J Phys Chem A* **113**: 3588–3593.
- Poulos T (1995) Cytochrome P450. *Curr Opin Struct Biol* **5**: 767–774.
- Rosenquist TA, Einolf HJ, Dickman KG, Wang L, Smith A and Grollman AP (2010). Cytochrome P450 1A2 detoxicates aristolochic acid in the mouse. *Drug Metab. Dispos.* **38**: 761–768.
- Sansen S, Yano JK, Reynald RL, Schoch GA, Griffin KJ, Stout CD, *et al.* (2007) Adaptations for the oxidation of polycyclic aromatic hydrocarbons exhibited by the structure of human P450 1A2. *J Biol Chem* **282**: 14348–14355.
- Shibusatani S, Bonala RR, Rosenquist T, Rieger R, Suzuki N, Johnson F, *et al.* (2010) Detoxification of aristolochic acid I by O-demethylation: less nephrotoxicity and genotoxicity of aristolochic acid Ia in rodents. *Int J Cancer* **127**: 1021–1027.
- Schmeiser HH, Bieler CA, Wiessler M, van Ypersele de Strihou C and Cosyns JP (1996) Detection of DNA adducts formed by aristolochic acid in renal tissue from patients with Chinese herbs nephropathy. *Cancer Res* **56**: 2025–2028.
- Schmeiser HH, Stiborova M and Arlt VM (2009) Chemical and molecular basis of the carcinogenicity of Aristolochia plants. *Curr Opin Drug Discov Devel* **12**: 141–148.
- Schwede T, Kopp J, Guex N and Peitsch MC (2003) SWISS-MODEL: An automated protein homology-modeling server. *Nucleic Acids Res* **31**: 3381–3385.
- Schyman P, Lai W, Chen H, Wang Y and Shaik S (2011) The directive of the protein: how does cytochrome P450 select the mechanism of dopamine formation? *J Am Chem Soc* **133**: 7977–7984.
- Sistkova J, Hudecek J, Hodek P, Frei E, Schmeiser HH and Stiborova M (2008) Human cytochromes P450 1A1 and 1A2 participate in detoxication of carcinogenic aristolochic acid. *Neuroendocrinol Lett* **29**: 733–737.
- Stiborova M, Frei E, Arlt VM and Schmeiser HH (2008a) Metabolic activation of carcinogenic aristolochic acid, a risk factor for Balkan endemic nephropathy. *Mutat Res* **658**: 55–67.
- Stiborova M, Frei E, Hodek P, Wiessler M and Schmeiser HH (2005) Human hepatic and renal microsomes, cytochromes P450 1A1/2, NADPH:cytochrome P450 reductase and prostaglandin H synthase mediate the formation of aristolochic acid-DNA adducts found in patients with urothelial cancer. *Int J Cancer* **113**: 189–197.

- 32 Stiborova M, Frei E and Schmeiser HH (2008b) Biotransformation enzymes in development of renal injury and urothelial cancer caused by aristolochic acid. *Kidney Int* **73**: 1209–1211.
- 33 Stiborova M, Frei E, Sopko B, Sopkova K, Markova V, Lankova M, *et al.* (2003) Human cytosolic enzymes involved in the metabolic activation of carcinogenic aristolochic acid: evidence for reductive activation by human NAD(P)H:quinone oxidoreductase. *Carcinogenesis* **24**: 1695–1703.
- 34 Stiborova M, Frei E, Wiessler M and Schmeiser HH (2001). Human enzymes involved in the metabolic activation of carcinogenic aristolochic acids: evidence for reductive activation by cytochromes P450 1A1 and 1A2. *Chem. Res. Toxicol.* **14**: 1128–1137.
- 35 Stiborova M, Levova K, Barta F, Shi Z, Frei E, Schmeiser HH, *et al.* (2012) Bioactivation versus detoxication of the urothelial carcinogen aristolochic acid I by human cytochrome P450 1A1 and 1A2. *Toxicol Sci* **125**: 345–358.
- 36 Stiborova M, Mares J, Frei E, Arlt VM, Martinek V and Schmeiser HH (2011a) The human carcinogen aristolochic acid I is activated to form DNA adducts by human NAD(P)H:quinone oxidoreductase without the contribution of acetyltransferases or sulfotransferases. *Environ Mol Mutagen* **52**: 448–459.
- 37 Stiborova M, Mares J, Levova K, Pavlickova J, Barta F, Hodek P, *et al.* (2011b) Role of cytochromes P450 in metabolism of carcinogenic aristolochic acid I: evidence of their contribution to aristolochic acid I detoxication and activation in rat liver. *Neuro Endocrinol Lett* **32** (Suppl 1): 121–130.
- 38 Stiborova M, Martinek V, Rydlova H, Hodek P and Frei E (2002) Sudan I is a potential carcinogen for humans: evidence for its metabolic activation and detoxication by human recombinant cytochrome P450 1A1 and liver microsomes. *Cancer Res.* **62**: 5678–5684.
- 39 Stiborova M, Martinek V, Schmeiser HH and Frei E (2006) Modulation of CYP1A1-mediated oxidation of carcinogenic azo dye Sudan I and its binding to DNA by cytochrome b₅. *Neuroendocrinol Lett* **27** Suppl 2: 35–39.
- 40 Stiborova M, Rupertova M and Frei E (2011c) Cytochrome P450- and peroxidase-mediated oxidation of anticancer alkaloid ellipticine dictates its anti-tumor efficiency. *Biochim Biophys Acta* **1814**: 175–185.
- 41 Vanherweghem JL, Depierreux M, Tielemans C, Abramowicz D, Dratwa M, Jadoul M, *et al.* (1993) Rapidly progressive interstitial renal fibrosis in young women: association with slimming regimen including Chinese herbs. *Lancet* **341**: 387–391.
- 42 Wang A, Savas U, Stout CD and Johnson EF (2011) Structural characterization of the complex between alpha-naphthoflavone and human cytochrome P450 1B1. *J Biol Chem* **286**: 5736–5743.
- 43 Xiao Y, Ge M, Xue X, Wang C, Wang H, Wu X, *et al.* (2008) Hepatic cytochrome P450s metabolize aristolochic acid and reduce its kidney toxicity. *Kidney Int* **73**: 1231–1239.
- 44 Yun BH, Rosenquist TA, Sidorenko V, Iden CR, Chen C-H, Pu Y-S, *et al.* (2012) Biomonitoring of aristolactam-DNA adducts in human tissues using ultra-performance liquid chromatography/ion-trap mass spectrometry. *Chem Res Toxicol* **25**: 1119–1131.